Journal of Power Sources 205 (2012) 80–85

Contents lists available at SciVerse ScienceDirect

Journal of Power Sources

journal homepage: www.elsevier.com/locate/jpowsour

Electrical and electrocatalytic properties of a $La_{0.8}Sr_{0.2}Co_{0.17}Mn_{0.83}O_{3-\delta}$ cathode for intermediate-temperature solid oxide fuel cells

Yaohui Bai[a,b,1], Mingfei Liu[a,1], Dong Ding[a], Kevin Blinn[a], Wentao Qin[a], Jiang Liu[b], Meilin Liu[a,*]

[a] Center for Innovative Fuel Cell and Battery Technologies, School of Materials Science and Engineering, Georgia Institute of Technology, 771 Ferst Drive, N.W., Atlanta, GA 30332, USA
[b] School of Chemistry and Chemical Engineering, South China University of Technology, Guangzhou 510641, Guangdong, People's Republic of China

ARTICLE INFO

Article history:
Received 15 October 2011
Received in revised form
16 December 2011
Accepted 1 January 2012
Available online 20 January 2012

Keywords:
Solid oxide fuel cell
Hybrid phase
Long-term stability

ABSTRACT

Our previous study of $La_{1-x}Sr_xMnO_{3\pm\delta}$ (LSM) infiltrated $La_{0.6}Sr_{0.4}Co_{0.2}Fe_{0.8}O_{3-\delta}$ (LSCF) cathode suggests that a hybrid phase, $La_{0.8}Sr_{0.2}Co_{0.17}Mn_{0.83}O_{3-\delta}$ (LSMCo), is associated with the observed enhancement in performance and stability of LSCF cathodes. Here we report the properties of LSMCo as a potential cathode for a solid oxide fuel cell (SOFC). The electrical conductivity of LSMCo varies from 118 to 166 S cm^{-1} at 500–800 °C. The interfacial polarization resistances of an LSMCo cathode on YSZ electrolyte are smaller than those of an LSM cathode at 600–800 °C. The performance of a cell based on an LSMCo cathode is ~34% higher than that based on an LSM cathode while maintaining comparable long-term stability, indicating that LSMCo is a promising cathode material for intermediate temperature SOFCs.

1. Introduction

Solid oxide fuel cells (SOFCs) have a great potential for efficient utilization of a wide variety of low-cost, readily available fuels [1–4]. However, cathode polarization still contributes considerably to energy loss in SOFC operation, more so at lower operating temperatures. While significant efforts have been devoted to the search for materials and architectures that are more active for O_2 reduction, $La_{1-x}Sr_xMnO_{3-\delta}$ (LSM) (>800 °C) and $La_{0.6}Sr_{0.4}Co_{0.2}Fe_{0.8}O_{3-\delta}$ (LSCF) (<750 °C) based cathodes still remain the most widely used ones because the adoption of alternative cathode materials is often hindered by unproven long-term stability and limited compatibility with YSZ electrolyte or other cell components, especially at high temperatures required for cell fabrication. It is well known that LSM has relatively high activity for O_2 reduction and good stability and compatibility with YSZ electrolyte at high temperatures [5–7]. Recently, DFT calculation showed that the Mn based cathodes have more favorable oxygen adsorption characteristics with rapid surface catalytic kinetics as opposed to the Co or Fe cations in $La_{1-x}Sr_xMO_{3-\delta}$ (where M = Mn, Co, or Fe) [8]. However, the performance of LSM is hindered by its extremely low oxygen ion conductivity at temperature below 800 °C, limiting the O_2 reduction reactions to the triple phase boundaries (TPB) between electrode, electrolyte and O_2 gas [5,6]. At lower operating temperatures, accordingly, LSCF-based cathodes showed higher performance than LSM-based ones, due most likely to the much higher ambipolar conductivity and the extension of active site for oxygen reduction beyond TPB [9]. However, the long-term stability of LSCF became a concern due primarily to Sr enrichment on LSCF surface [10,11]. It is desirable, therefore, to modify the surface of LSCF cathodes for enhanced stability and better performance.

One effective approach is to modify the surface of LSCF cathodes by a thin-film coating of a catalyst with higher stability and catalytic activity toward oxygen reduction. A successful example is a cathode consisting of a porous LSCF backbone and a thin coating of LSM [12]. The LSM-infiltrated LSCF allows the use of the best properties of two different materials: the excellent ambipolar conductivity of LSCF and the high stability and catalytic activity of LSM. The catalyst coating could be a porous layer of discrete particles or a dense, continuous film. Nanoparticles of ionic conductors such as SDC have been successfully deposited on LSCF surface by infiltration of aqueous nitrate solutions [13,14]. In contrast, dense films of LSM have been prepared using non-aqueous solutions [15]. The challenges lie in how to achieve rational design of desired architecture and microstructure for each component with reduced polarization and enhanced stability at low cost. Recently, the infiltration of a thin LSM coating on a porous LSCF cathode had successfully enhanced both the performance and the stability of the LSCF cathode [16]. Careful characterization of the LSM coating on LSCF after annealing at 850 °C for 900 h revealed that Co diffused from the underlying LSCF into the LSM layer to form a hybrid phase between LSM and LSCF. However, there was no evidence of strontium enrichment or

* Corresponding author. Tel.: +1 404 894 6114; fax: +1 404 894 9140.
E-mail address: meilin.liu@mse.gatech.edu (M. Liu).
[1] These authors contributed equally to this work.

0378-7753/$ – see front matter © 2012 Elsevier B.V. All rights reserved.
doi:10.1016/j.jpowsour.2012.01.021

surface phase (e.g., SrO) segregation [15,16]. Further, microanalyses of the LSM layer on LSCF performed under TEM suggested that the composition of the hybrid phase is $La_{0.8}Sr_{0.2}Co_{0.17}Mn_{0.83}O_{3-\delta}$ (LSMCo), which is responsible for the observed enhancement in performance and stability of LSCF cathodes. Hence, it is important to evaluate the intrinsic properties of the LSMCo cathode under typical fuel cell operating conditions. In fact, there have been several reports focused on the study of Co-doped LSM materials. For example, Kuharuangrong et al. [17] studied the thermal expansion coefficients (TEC) and electrical conductivities of $La_{0.84}Sr_{0.16}Mn_{0.6}Co_{0.4}O_3$ and $La_{0.84}Sr_{0.16}Mn_{0.8}Co_{0.2}O_3$. They found that the electrical conductivity of the Co-doped LSM decreases but the TEC increases slightly with the amount of Co. The TEC for $La_{0.84}Sr_{0.16}Mn_{0.8}Co_{0.2}O_3$ ($\sim 11.69 \times 10^{-6}\,K^{-1}$) is close to that of YSZ ($10.3 \times 10^{-6}\,K^{-1}$) [18]. Badwal et al. [19,20] reported the chemical diffusion coefficient of Co in LSM and the application of work function measurement for surface monitoring of the (La,Sr)(Mn,Co)O_3. Huang et al. [21] impregnated $La_{0.8}Sr_{0.2}Mn_{(1-x)}Co_xO_3$ ($x = 0$, 0.1, 0.25 and 0.5) into a scaffold of YSZ to form composite cathodes and examined their electrochemical performance. They found that the performance was the best when the content of Co was ~25%. However, limited data are available for $La_{0.8}Sr_{0.2}Co_{0.17}Mn_{0.83}O_{3-\delta}$, which is the most stable composition for LSM-infiltrated LSCF cathodes with high performance and excellent stability.

In the present study, we have systematically characterized the crystal structure, phase stability, electrical conductivity, and compatibility with YSZ electrolyte of LSMCo. Further, electro-catalytic activity for oxygen reduction of LSMCo as cathode for YSZ-based fuel cells was also evaluated under typical fuel cell operating conditions.

2. Experimental

$La_{0.8}Sr_{0.2}MnO_{3-\delta}$ (LSM) and $La_{0.8}Sr_{0.2}Co_{0.17}Mn_{0.83}O_{3-\delta}$ (LSMCo) powders were synthesized using a micro-wave assisted sol–gel method. Take LSMCo for example: stoichiometric amounts of analytic grade $La(NO_3)_3{\cdot}6H_2O$, $Sr(NO_3)_2$, $Mn(NO_3)_2{\cdot}4H_2O$ and $Co(NO_3)_2{\cdot}6H_2O$ were dissolved in an aqueous solution, and citric acid were then added to serve as the complexing agents. The molar ratio of total metal ions to citric acid was kept at 1:1.5. The solution was then heated in a microwave oven (Panasonic NN-H765WF, 1250 W) for 10 min to get gelation. The resulted gel was held at 150 °C for 24 h to remove additional water, and then calcined at 500–800 °C for 2 h. The as-prepared powders were uniaxially pressed into pellets under a pressure of 375 MPa and subsequently sintered at 1350 °C for 7 h to get dense pellets. To investigate the chemical compatibility between LSMCo and YSZ electrolyte, LSMCo was mixed with YSZ (Tosoh, Japan) at 1:1 weight ratio and then fired in air at 1050–1150 °C for 5 h. To investigate the electrochemical behavior of the LSM and LSMCo cathode, both symmetric cells and anode supported cells were fabricated as described as follows [22]. The symmetrical cells were constructed with YSZ electrolyte as the substrates to measure the interfacial polarization resistance under open circuit conditions or under cathodic polarization. The substrates were prepared by dry pressing YSZ powder, followed sintering at 1450 °C for 5 h to get dense YSZ pellets (~10.7 mm in diameter and ~0.6 mm in thickness). LSM and LSMCo slurries, prepared by mixing the as-prepared powders with organic binder (Heraeus V006) and acetone, were brush painted on both surfaces of electrolyte pellets and fired at 1050 °C for 2 h to form symmetric cells. A silver reference electrode (RE) was then positioned close to the working electrode (WE) for three-electrode electrochemical measurements.

The anode-supported single cells with YSZ as the electrolytes and Ni–YSZ as the anodes were fabricated to further characterize the electrode performance. Ni–YSZ anode support was tape casted and pre-fired at 900 °C for 2 h, then an active NiO–YSZ layer (~15 μm) and YSZ electrolyte (~15 μm) were sequentially deposited on the anode support by a particle suspension coating processes [23,24] followed by co-firing at 1400 °C for 5 h. The cathode was then applied to the YSZ electrolyte using the same procedures for the fabrication of symmetric cells as described earlier.

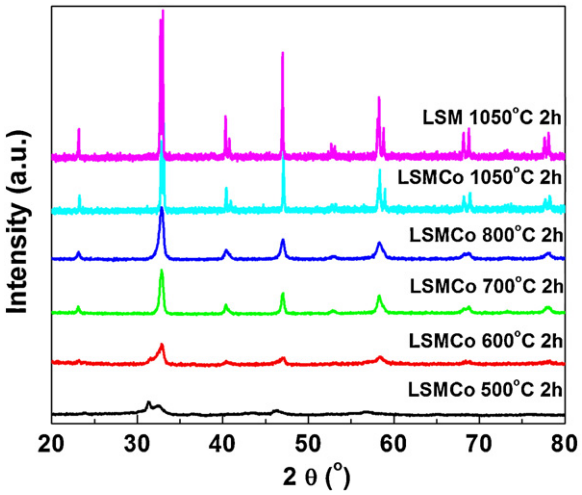

Fig. 1. XRD patterns of LSMCo powders calcined at different temperatures.

X-ray diffraction analysis (X' Pert PRO Alpha-1 PW-1800X-ray diffractometer with Cu Kα radiation) and Raman spectroscopy (Renishaw 1000, 633 nm excitation) were used for phase identification. The conductivities of the LSM and LSMCo cathodes were measured using a Van der Pauw method [25]. Impedance measurements were performed using a Solartron 1255 HF frequency response analyzer, interfaced with an EG&G PAR potentiostat model 273A with an amplitude of 10 mV in the frequency range from 100 kHz to 0.1 Hz. For the stability test, the anode supported cell was mounted and sealed on a fuel cell testing fixture, and then tested with 3 vol.% water humidified hydrogen (30 ml min^{-1}) as fuel and ambient air as oxidant. The cell performances and the long-term electrochemical performances of test cells were examined with an Arbin multi-channel electrochemical testing system (MSTAT). Microstructure of the cathodes was observed by scanning electron microscopy (SEM, LEO 1530).

3. Results and discussion

3.1. Phase formation of LSMCo powders and chemical compatibility with YSZ electrolyte

XRD patterns of LSMCo powders calcined at different temperatures (Fig. 1) suggest that perovskite structure started to form at 600 °C. As increasing the firing temperature, the characteristic XRD peaks became sharper and sharper, indicating the grain growth and improvement of the crystallinity of the perovskite phase. The grain sizes, determined from the Scherrer formula using the (1 1 0) peak, were 22, 32, 45, and 99 nm at firing temperatures of 600, 700, 800, 1050 °C, respectively. Monoclinic perovskite structure was formed when LSMCo was fired at 1050 °C for 2 h. Kuharuangrong et al. [17] reported the formation of monoclinic perovskite $La_{0.84}Sr_{0.16}Mn_{0.8}Co_{0.2}O_3$ and $La_{0.84}Sr_{0.16}Mn_{0.6}Co_{0.4}O_3$ fired at 1200 °C. This suggests that the powders from the present work have higher reactivity. The lattice parameters of LSMCo fired at 1050 °C are $a = 5.4308$ Å, $b = 5.4987$ Å, $c = 7.6393$ Å and $\beta = 90.2368$. For comparison, the XRD pattern of LSM was also presented in Fig. 1. It can be seen that the diffraction peaks of LSMCo shift slightly

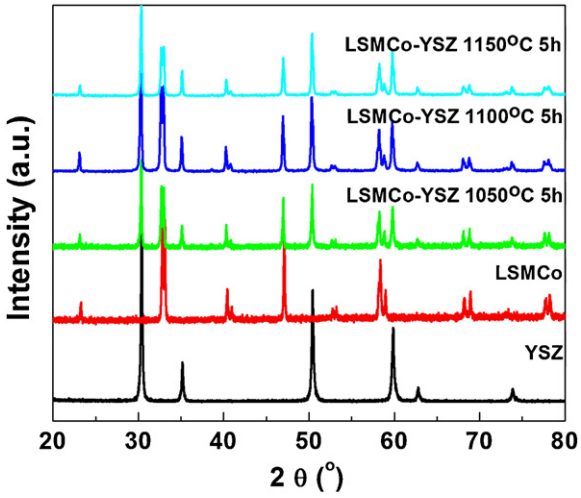

Fig. 2. XRD patterns of LSMCo–YSZ powder mixtures fired at different temperatures.

to larger angle when compared with those of LSM, indicating a decrease in the lattice constant. Kuharuangrong et al. [17] also reported that the lattice parameters decreased with Co content in LSM because the size of Co^{3+} is smaller than that of Mn^{3+}.

While LSM is compatible with YSZ electrolyte [26], the compatibility between Co doped LSM and YSZ depends on the Co doping level [21]. Solid state reaction between $La_{0.8}Sr_{0.2}Co_xMn_{(1-x)}O_3$ ($x = 0.25$ and 0.5) and YSZ was observed when co-fired at 1100 °C while $La_{0.8}Sr_{0.2}Co_{0.1}M_{0.9}O_3$ was chemically compatible with YSZ [21]. Thus, it is necessary to investigate the chemical compatibility between LSMCo and YSZ. Fig. 2 shows the XRD patterns from mixtures of LSMCo and YSZ fired at different temperatures for 5 h. When fired at 1050–1150 °C for 5 h, no observable secondary phases were formed between LSMCo and YSZ, indicating that $La_{0.8}Sr_{0.2}Co_xMn_{(1-x)}O_3$ ($x = 0.17$) is chemically compatible with the YSZ electrolyte. However, from Fig. 3, we can see that a peak at 302 cm^{-1} appeared in the Raman spectra obtained from a LSMCo–YSZ mixture fired at 1200 °C, suggesting that a reaction product $La_2Zr_2O_7$ was formed between LSMCo and YSZ [27]. This peak was absent from the spectra of the samples fired at lower temperatures, indicating that LSMCo and YSZ are chemically compatible at these temperatures. Accordingly, LSMCo can be directly fired on YSZ electrolyte at 1050 °C for 2 h without the need for a doped ceria buffer layer.

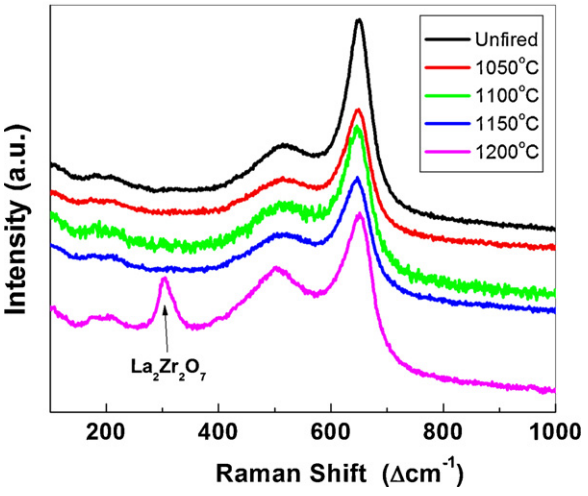

Fig. 3. Raman spectra of LSMCo–YSZ powder mixtures fired at different temperatures.

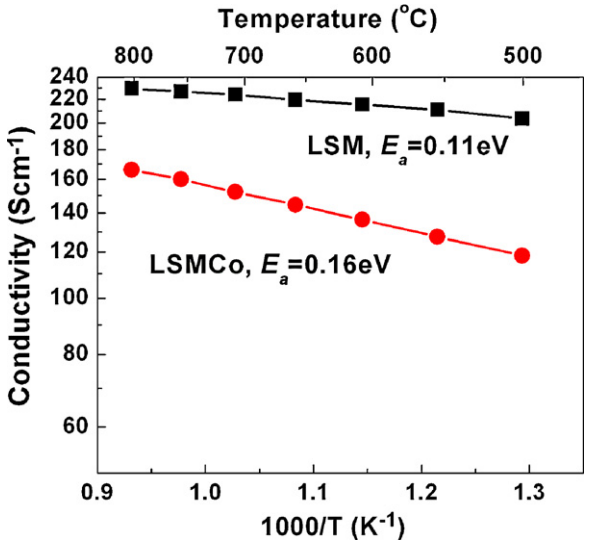

Fig. 4. Electrical conductivities of LSM and LSMCo in the temperature range of 500–800 °C.

3.2. Electrical conductivities

Fig. 4 shows the temperature dependence of the electrical conductivities (σ) of LSM and LSMCo. The conductivities of the LSM without Co varied from 203 to 229 S cm^{-1} in the temperature range of 500–800 °C, which are slightly higher than those of the LSMCo (118–166 S cm^{-1} at 500–800 °C). The decrease in electrical conductivity of LSMCo compared with LSM can be explained by electron–hole charge compensation. While the conductivity of lanthanum strontium manganite is determined by hole-hopping conduction, that of lanthanum strontium cobaltite is dominated by electron transport [17,28]. Thus, the electrons associated with the doping of 17 mol% Co might combine with the holes in the host lanthanum strontium manganite, reducing the net charge carriers density and hence the conductivity of LSMCo. It is also noted that the activation energies for LSM (0.11 eV) is lower than that for LSMCo (0.16 eV), which is consistent with the report by Kuharuangrong et al. [17] and Tai et al. [29].

3.3. Electrochemical performance under open circuit conditions

Fig. 5 shows the interfacial polarization resistance (R_p) of LSM and LSMCo cathodes on YSZ electrolyte at 600–800 °C measured under open circuit conditions (OCV). Clearly, the R_p for LSMCo were smaller than those for LSM in the testing temperature range. For example, the R_p at 750 °C was reduced from 35.0 Ω cm^2 for LSM to 24.8 Ω cm^2 for LSMCo, representing a 29.1% improvement. Therefore, LSMCo exhibited higher electrocatalytic activity than LSM toward oxygen reduction reactions.

3.4. Activation behaviors

It is well known that LSM-based cathodes can be activated significantly by the application of a cathodic polarization [30,31]. Such an activation behavior of LSM-based cathodes was attributed to the broadening of the TPBs as a result of an increase in local oxygen vacancy concentration induced by cathodic polarization [32]. To investigate the activation behavior of LSMCo cathodes, we used a symmetrical test cell with a three-electrode configuration. The use of a reference electrode enable us to separate the cathodic from the anodic polarization at a given cell voltage applied between the working and the reference electrodes. All electrochemical measurements under a polarized condition were collected at lease 30 min

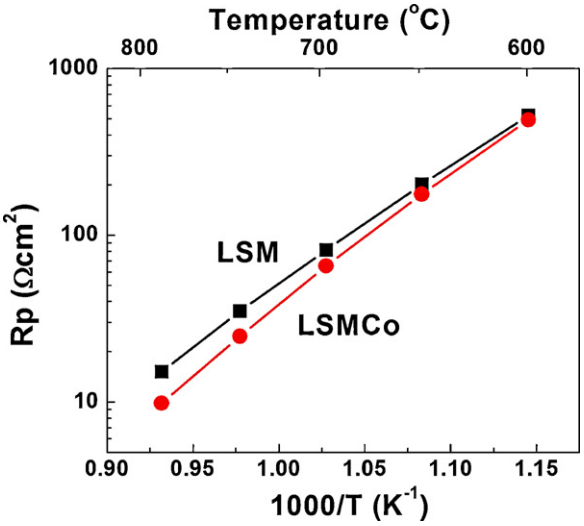

Fig. 5. Interfacial polarization resistance for LSM and LSMCo electrodes on a YSZ electrolyte as determined from impedance spectroscopy at 600–800 °C.

after a steady state was reached. Fig. 6 shows the impedance spectra for cells with LSM and LSMCo cathodes at 750 °C under different cathodic polarizations. As we can see, both LSM and LSMCo cathodes showed obvious activation process. The R_p of the LSM cathodes decreased from 35.1 to 2.8 Ω cm^2 while the R_p of the LSMCo cathodes decreased from 21.5 to 2.4 Ω cm^2 when −0.3 V was applied, indicating that the LSMCo cathode has a similar activation behavior as the LSM cathode. Shown in Fig. 7 are some typical polarization curves for the two types of cathodes obtained at 750 °C. The overpotentials (η) were calculated from the following equation:

$$\eta = U_{WR} - iR_{ohm} \quad (1)$$

where U_{WR} is the applied voltage, i is the current, and R_{ohm} is the ohmic resistance of the test cell determined from impedance spectroscopy performed under the same conditions. The overpotentials for the LSMCo cathodes are a little bit smaller than those for the LSM cathodes at each current density; the difference in overpotential appeared to increase with current density, implying that the LSMCo cathode may perform better than the LSM cathode under typical fuel cell operation conditions.

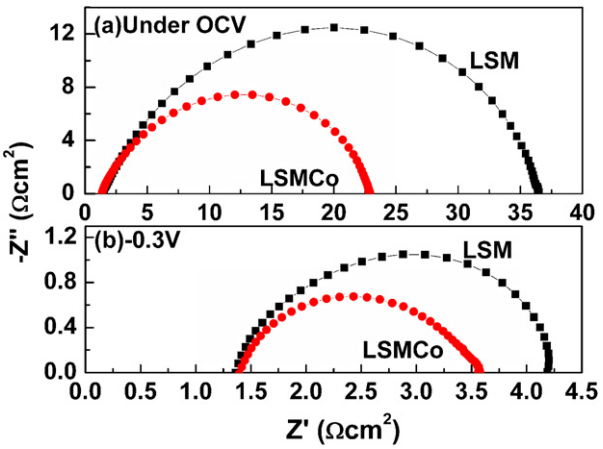

Fig. 6. Impedance spectra for LSM and LSMCo electrodes on an YSZ electrolyte at 750 °C under (a) OCV condition and (b) a cathodic bias of −0.3 V.

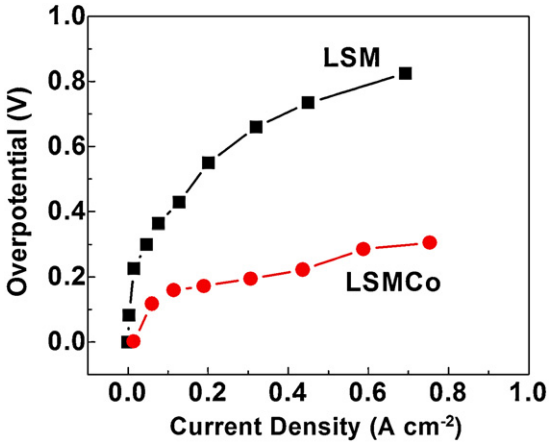

Fig. 7. Cathodic polarization curves (overpotential η versus current density i) for LSM and LSMCo electrodes on an YSZ electrolyte.

3.5. Long-term stability of single cells with LSM and LSMCo cathode

As discussed earlier, the long term stability and compatibility with YSZ electrolyte is often the main concern for a new cathode material. For example, while the short-term performance of an LSCF cathode can be nearly twice that of an LSM cathode [33], the degradation in power density has been reported to 0.06–0.17% h^{-1} for anode-supported YSZ cells with LSCF cathode operated at 750 °C and 0.7 V [34]. Fig. 8 shows the time dependence of performance for single cells with LSM and LSMCo as the cathode deposited on YSZ electrolyte (~15 μm thick) supported by Ni–YSZ anode. Humidified hydrogen (~3% H_2O) was used as the fuel and ambient air as the oxidant. After about 100 h operation at 750 °C under 0.7 V, the current densities of the cells with LSM and LSMCo cathode approached ~0.50 and ~0.67 A cm^{-2}, respectively, without any sign of degradation for both. The performance of the cell with the LSMCo cathode is ~34% higher than that of the LSM cathode while maintaining comparable stability, suggesting that the LSMCo is a promising cathode material for intermediate temperature SOFCs. The observed enhancement in power output and stability is attributed to the suppression of SrO formation on cathode surface and the increase in local oxygen vacancies by cathodic polarization [31]. It is noted that the initial activation of the LSMCo cathode is faster than that of the LSM cathode: it took ~30 h for

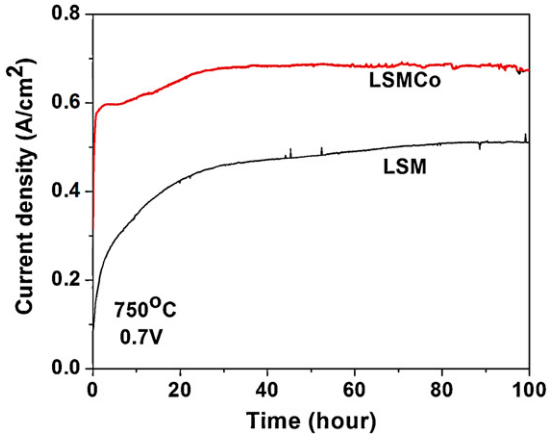

Fig. 8. Stability of single cells with LSM and LSMCo cathodes as measured at 750 °C under a constant cell voltage of 0.7 V using humidified hydrogen as the fuel and stationary air as the oxidant (cell configuration: Ni–YSZ/YSZ/cathode).

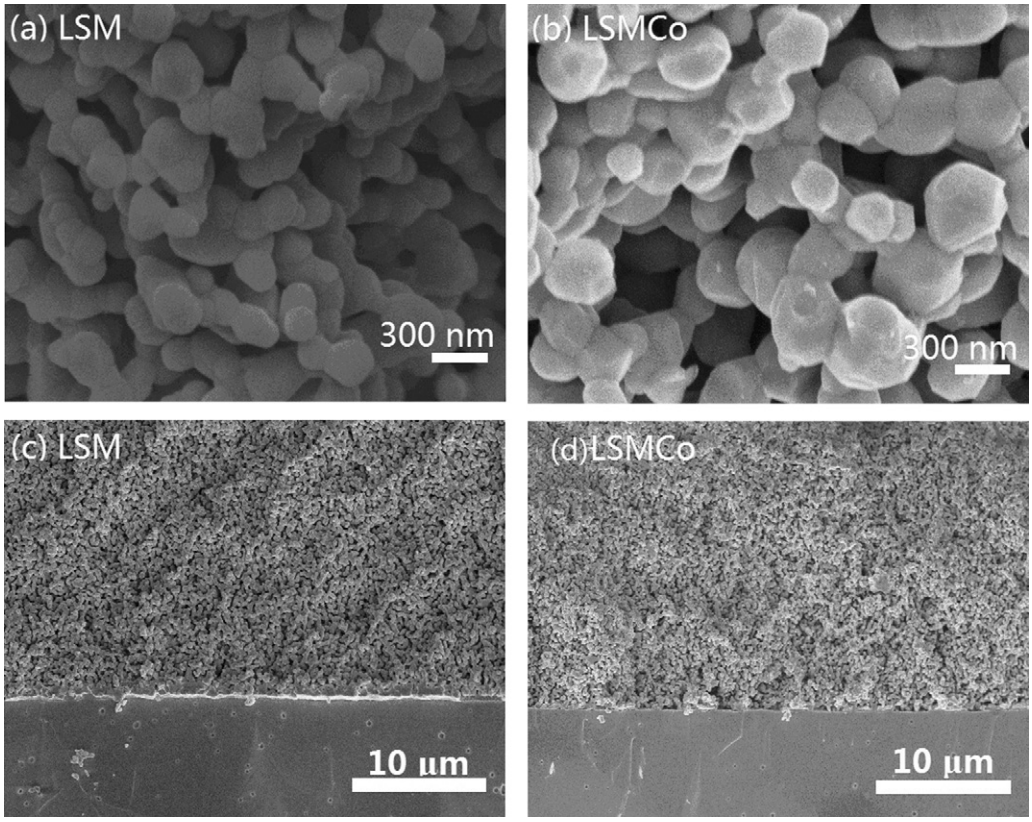

Fig. 9. Cross-sectional views (SEM images) of (a, c) LSM and (b, d) LSMCo cathodes on an YSZ electrolyte after testing at 750 °C for 100 h.

the LSMCo cathode to reach the steady state but ~70 h for the LSM cathode.

3.6. Microstructure of LSM and LSMCo cathode

Fig. 9 shows some typical microstructures of the LSM and LSMCo cathode and the interfaces between the electrolyte and the cathodes after testing. Both LSM and LSMCo cathodes have similar uniform and porous structure (~40% porosity) and adhered well to the electrolyte. It indicates that the brush painting method is reliable and available for preparing cathode and the difference of performances between LSM and LSMCo caused by the fabrication process is negligible. While their microstructures are similar, the grain sizes of the LSM cathode are slightly smaller than those of the LSMCo cathode: 0.2–0.3 μm for LSM (Fig. 9a) and 0.3–0.4 μm for LSMCo (Fig. 9b).

4. Conclusions

$La_{0.8}Sr_{0.2}Co_{0.17}Mn_{0.83}O_{3-\delta}$ is examined as a potential cathode material for SOFCs. XRD analysis shows that LSMCo is chemically compatible with YSZ electrolyte up to 1150 °C. Its electrical conductivity varies from 118 to 166 S cm^{-1} in the temperature range of 500–800 °C, suitable as cathode for intermediate temperature SOFCs. Electrochemical measurements demonstrate that the interfacial polarization resistance of LSMCo on YSZ electrolyte is smaller than that of LSM in the temperature range of 600–800 °C and the overpotential of LSMCo is smaller than that of LSM under fuel cell operation conditions. The performance of LSMCo is ~34% higher than that of LSM when they are used as cathode in single cells operated at 750 °C at 0.7 V. No obvious degradation is observed for the LSMCo cathode after operation for 100 h.

Acknowledgments

This work was supported by the U.S. Department of Energy SECA Core Technology Program under award number DE-NT0006557. Yaohui Bai thanks the fellowship support by the China Scholarship Council (CSC).

References

[1] N.Q. Minh, J. Am. Ceram. Soc. 76 (1993) 563–588.
[2] L. Yang, S.Z. Wang, K. Blinn, M.F. Liu, Z. Liu, Z. Cheng, M.L. Liu, Science 326 (2009) 126–129.
[3] L. Yang, Y. Choi, W. Qin, H. Chen, K. Blinn, M. Liu, P. Liu, J. Bai, T.A. Tyson, M. Liu, Nat. Commun. 2 (2011) 357.
[4] Z. Cheng, J.-H. Wang, Y. Choi, L. Yang, M.C. Lin, M. Liu, Energy Environ. Sci. 4 (2011) 4380–4409.
[5] C. Lee, S.W. Baek, J. Bae, Solid State Ionics 179 (2008) 1465–1469.
[6] S.P. Jiang, W. Wang, Solid State Ionics 176 (2005) 1351–1357.
[7] R.F. Tian, J. Fan, Y. Liu, C.R. Xia, J. Power Sources 185 (2008) 1247–1251.
[8] Y. Choi, M.C. Lin, M. Liu, J. Power Sources 195 (2010) 1441–1445.
[9] H. Yokokawa, N. Sakai, T. Horita, K. Yamaji, M.E. Brito, H. Kishimoto, J. Alloys Compd. 452 (2008) 41–47.
[10] N.P. Xu, S.G. Li, W.Q. Jin, P. Huang, J. Shi, Y.S. Lin, J. Membr. Sci. 166 (2000) 51–61.
[11] S.P. Simner, M.D. Anderson, M.H. Engelhard, J.W. Stevenson, Electrochem. Solid-State Lett. 9 (2006) A478–A481.
[12] M.L. Liu, Z. Liu, M.F. Liu, L.F. Nie, D.S. Mebane, D.S. Wilson, W. Surdoval, US Patent Application No. 12/837,757 (2010).
[13] L. Nie, M. Liu, Y. Zhang, M. Liu, J. Power Sources 195 (2010) 4704–4708.
[14] X. Lou, Z. Liu, S. Wang, Y. Xiu, C.P. Wong, M. Liu, J. Power Sources 195 (2010) 419–424.
[15] J.-J. Choi, W. Qin, M. Liu, M. Liu, J. Am. Ceram. Soc. 94 (2011) 3340–3345.
[16] M.E. Lynch, L. Yang, W. Qin, J.-J. Choi, M. Liu, K. Blinn, M. Liu, Energy Environ. Sci. 4 (2011) 2249–2258.
[17] S. Kuharuangrong, T. Dechakupt, P. Aungkavattana, Mater. Lett. 58 (2004) 1964–1970.
[18] J. Schoonman, J.P. Dekker, J.W. Broers, N.J. Kiwiet, Solid State Ionics 46 (1991) 299–308.
[19] S.P.S. Badwal, S.P. Jiang, J. Love, J. Nowotny, M. Rekas, E.R. Vance, Ceram. Int. 27 (2001) 419–429.
[20] S.P.S. Badwal, T. Bak, S.P. Jiang, J. Love, J. Nowotny, M. Rekas, C.C. Sorrell, E.R. Vance, J. Phys. Chem. Solids 62 (2001) 723–729.

[21] Y.Y. Huang, J.M. Vohs, R.J. Gorte, J. Electrochem. Soc. 153 (2006) A951–A955.
[22] C.R. Xia, B.B. Liu, Z.Y. Jiang, B. Ding, F.L. Chen, J. Power Sources 196 (2011) 999–1005.
[23] M.F. Liu, D.H. Dong, R.R. Peng, J.F. Gao, J. Diwu, X.Q. Liu, G.Y. Meng, J. Power Sources 180 (2008) 215–220.
[24] M.F. Liu, J.F. Gao, D.H. Dong, X.Q. Liu, G.Y. Meng, Int. J. Hydrogen Energy 35 (2010) 10489–10494.
[25] L.J. Van der Pauw, Philips Tech. Rev. 20 (1958) 220–224.
[26] I. Yasuda, M. Hishinuma, J. Solid State Chem. 123 (1996) 382–390.
[27] L.D. Lu, Y.P. Tong, Y.P. Wang, Z.X. Yu, X. Wang, X.J. Yang, Mater. Lett. 62 (2008) 889–891.
[28] S. Carter, A. Selcuk, R.J. Chater, J. Kajda, J.A. Kilner, B.C.H. Steele, Solid State Ionics 53–56 (1992) 597–605.
[29] L.W. Tai, M.M. Nasrallah, H.U. Anderson, D.M. Sparlin, S.R. Sehlin, Solid State Ionics 76 (1995) 259–271.
[30] Y. Jiang, S.Z. Wang, Y.H. Zhang, J.W. Yan, W.Z. Li, J. Electrochem. Soc. 145 (1998) 373–378.
[31] S.P. Jiang, J. Solid State Electrochem. 11 (2006) 93–102.
[32] W. Wang, S.P. Jiang, J. Solid State Electrochem. 8 (2004) 914–922.
[33] A. Mai, V.A.C. Haanappel, S. Uhlenbruck, F. Tietz, D. Stover, Solid State Ionics 176 (2005) 1341–1350.
[34] J.Y. Kim, V.L. Sprenkle, N.L. Canfield, K.D. Meinhardt, L.A. Chick, J. Electrochem. Soc. 153 (2006) A880–A886.